

Persistence and survival in equilibrium step fluctuations

M. Constantin¹, C. Dasgupta², S. Das Sarma³, D. B. Dougherty⁴, and E. D. Williams⁵

¹ Department of Physics and Astronomy, University of California, Irvine, CA 92697-4575, USA

E-mail: magda@uci.edu

² Centre for Condensed Matter Theory, Department of Physics, Indian Institute of Science, Bangalore 560012, India

E-mail: cdgupta@physics.iisc.ernet.in

³ Condensed Matter Theory Center, Department of Physics, University of Maryland, College Park, MD 20742-4111, USA

E-mail: dassarma@physics.umd.edu

⁴ Surface and Microanalysis Science Division, NIST, 100 Bureau Dr., Mailstop 8372, Gaithersburg, MD 20899-8372, USA

E-mail: dougherty.daniel@gmail.com

⁵ Department of Physics and MRSEC, University of Maryland, College Park, MD 20742-4111, USA

E-mail: edw@umd.edu

Abstract. Results of analytic and numerical investigations of first-passage properties of equilibrium fluctuations of monatomic steps on a vicinal surface are reviewed. Both temporal and spatial persistence and survival probabilities, as well as the probability of persistent large deviations are considered. Results of experiments in which dynamical scanning tunneling microscopy is used to evaluate these first-passage properties for steps with different microscopic mechanisms of mass transport are also presented and interpreted in terms of theoretical predictions for appropriate models. Effects of discrete sampling, finite system size and finite observation time, which are important in understanding the results of experiments and simulations, are discussed.

PACS numbers: 05.40.-a, 05.70.Np, 68.35.Ja, 68.37.Ef

1. Introduction

Many problems in physics require understanding the stochastic dynamics of spatially extended objects. Traditionally, the equilibrium and nonequilibrium dynamical properties of such systems have been described in terms of space- and time-dependent correlation functions. In recent years, there has been considerable interest in studies of first-passage properties [1, 2] of the dynamical fluctuations of such objects, quantified in terms of *persistence* and *survival* probabilities. The first-passage problem for a temporally fluctuating quantity involves determining the distribution of times for the quantity to cross a specified reference value *for the first time*. The persistence probability, defined as the probability of the stochastic variable *not* returning to its initial value in a specified time interval, is essentially an integral of the distribution of the corresponding first-passage time. A closely related quantity, the survival probability, measures the probability of not crossing some other reference point, such as the average value of the stochastic process, in a specified time interval. These probabilities depend on the whole history of the time evolution of the system in the specified time interval, and provide a characterization of the underlying stochastic dynamics that is complementary to, and in some sense more detailed than a description based on correlation functions.

Persistence and survival probabilities have been used in recent years to describe the statistics of first-passage events in a variety of spatially extended stochastic systems. Examples of such applications range from the classical diffusion equation [3] to the zero-temperature dynamics of ferromagnetic Ising and Potts models [4, 5], nonequilibrium critical dynamics [6], reaction-diffusion processes in disordered environments [7], and volatility in stock market fluctuations [8]. An increasing number of experimental results are also available for persistence and survival in systems such as coalescence of droplets [9], coarsening of two-dimensional soap froth [10], twisted nematic liquid crystal [11], nuclear spin distribution in laser-polarized atomic gas [12], and slow combustion front in paper [13].

There also has been much recent interest in experimental and theoretical studies of the stochastic dynamics of growth and fluctuation of structures on surfaces [14, 15, 16, 17]. The technique of imaging spatial distributions and temporal variations of structures on surfaces using scanning tunneling microscopy (STM) has made it possible to perform experiments in which theoretical predictions can be tested directly. Equilibrium fluctuations of crystal layer boundaries or *steps* on a vicinal surface, obtained by cutting a crystal in a direction close to a high-symmetry plane, have been extensively studied [18, 19] in this context. A vicinal surface consists of an array of monatomic steps separated by terraces of the high-symmetry plane. In thermal equilibrium, which can be achieved in experiments if the temperature is sufficiently high, the one-dimensional (1d) steps roughen due to thermal fluctuations. The stochastic dynamics of these fluctuations is theoretically modeled by Langevin equations [15, 18, 19] and atomistic, solid-on-solid models [15]. Theoretical and experimental investigations [18, 19] of various space- and time-dependent correlation functions of equilibrium step fluctuations have provided a

wealth of information about the physical parameters that govern these fluctuations.

In this paper, we review the results of our recent analytic, numerical and experimental investigations [20, 21, 22, 23, 24, 25, 26, 27, 28, 29, 30, 31, 32] of various first-passage properties of equilibrium step fluctuations. In these studies, both temporal and spatial persistence and survival probabilities of different kinds are considered and the results of STM experiments on systems with different microscopic mechanisms of step-edge fluctuations are compared directly with the predictions of analytic and numerical calculations for appropriate models. The first studies of first-passage statistics of surface growth and fluctuations were carried out by Krug and co-workers [33, 34] who obtained analytic and numerical results for the persistence probability for several Langevin equations for interface dynamics. Our work addresses many other interesting questions about the first-passage statistics of interface fluctuations. The motivation for these studies arises partly from the possibility of making direct comparisons between experimental observations and theoretical predictions for various first-passage properties of these systems. Such comparisons provide an opportunity to validate the theoretical models commonly used to describe step fluctuations. As noted in Ref. [35], a description of dynamical interface fluctuations in terms of persistence and survival probabilities is not just an equivalent alternative to the usual description [14, 15, 16] based on dynamical scaling: first-passage properties provide a richer characterization of the fully nonlocal and non-Markovian (both in space and time) nature of interface fluctuations. This is reflected in the nontrivial behavior of some of the first-passage properties even for fluctuation processes described by linear dynamical equations for which dynamical scaling is rather trivial [35].

Our studies are also motivated by the importance of step fluctuations in the practical problem of assessing the stability of nanoscale structures. This is a fundamental and challenging issue that will become increasingly important as the length scale of devices approaches the atomic limit [36, 37, 38]. In this context, it is important to address questions such as what is the distribution of the time for a nanoscale structure to fluctuate *for the first time* to a point of encounter at which a change in properties or some other switching behavior may occur. Studies of first-passage properties of fluctuating steps and similar atomic-scale structures on surfaces are relevant for answering such questions.

The rest of this paper is organized as follows. Various persistence and survival properties studied by us are defined in section 2. The models used in our analytic and numerical studies are defined in section 3. The methods used in our numerical studies are also summarized in this section. Section 4 contains a brief account of our experimental methods. The results of our analytic, numerical and experimental studies of first-passage properties of equilibrium fluctuations of isolated steps with different microscopic kinetics are described in detail in section 5. Section 6 contains a summary of our main results and a few concluding remarks.

2. Persistence and survival probabilities

We consider an isolated 1d step whose position at time t is described by the function $h(x, t)$ where the x -axis is taken to be along the average step position. In temporal persistence and survival, we consider the temporal fluctuations of $h(x, t)$ at a fixed position x . The temporal persistence probability $P(x; t_0, t_0 + t)$ is defined as the probability that the sign of $[h(x, t_0 + t') - h(x, t_0)]$ *does not change* for *all* $0 < t' \leq t$. Clearly, this is the probability that the step-edge position does not return to its initial value (at time t_0) during its stochastic time evolution over the period from t_0 to $t_0 + t$. Averaging $P(x; t_0, t_0 + t)$ over the coordinate x and the initial time t_0 in the equilibrium state of the step, one obtains the temporal persistence probability $P(t)$ considered in our work. It is obvious that $P(t)$ is closely related to the zero-crossing statistics of the stochastic variable $[h(x, t_0 + t) - h(x, t_0)]$. In particular, if $w(t)$ is the distribution of the time interval between two successive zero crossings of this quantity, then $P(t) = \int_t^\infty w(t') dt'$.

The probability of *persistent large deviations*, introduced by Dornic and Godreche [39], provides a more detailed characterization of stochastic processes. A closely related idea, that of sign-time distribution, was developed in Ref. [40]. This involves the variable $r(t) \equiv \text{sign}[h(x, t_0 + t) - h(x, t_0)]$ that takes the values ± 1 . The average sign variable $r_{av}(t)$ is defined as $r_{av}(t) \equiv t^{-1} \int_0^t r(t') dt'$. Clearly, the values of $r_{av}(t)$ lie between -1 and 1 . Then, the probability of persistent large deviations, $P(t, s)$, is defined as the probability for the average sign r_{av} to remain above a certain pre-assigned value s ($-1 \leq s \leq 1$), up to time t : $P(t, s) \equiv \text{Prob} \{ r_{av}(t') \geq s, \forall 0 < t' \leq t \}$. Averages over the initial time t_0 and the coordinate x are implied in the above definition. Also, we assume, without any loss of generality, that the initial deviation of the step position is in the “positive” direction, i.e. $h(x, t_0 + t) > h(x, t_0)$ for $t \rightarrow 0$. Then, the initial value of $r_{av}(t)$ is equal to unity and $P(t, s = 1)$ is identical to the temporal persistence probability $P(t)$ defined above. Also, $P(t, s = -1)$ is trivially equal to unity for all t . The time-dependence of $P(t, s)$ for $-1 < s < 1$ is quite nontrivial and its dependence on s provides a convenient way of characterizing the underlying stochastic dynamics.

The temporal survival probability $S(x; t_0, t_0 + t)$ is defined as the probability that the sign of $[h(x, t_0 + t') - \bar{h}]$ *does not change* for *all* $0 < t' \leq t$. Here, \bar{h} is the *thermodynamic average* value of the step position which does not depend on the coordinate x . Thus, the temporal survival probability $S(t)$, obtained by averaging $S(x; t_0, t_0 + t)$ over t_0 and x , measures the probability of the step position not crossing its average value during its evolution over time t . This quantity is clearly related to the zero crossing statistics of the deviation of the step position from its average value. Although the definition of $S(t)$ is rather similar to that of the persistence probability $P(t)$, the time-dependences of these two quantities turn out to be quite different.

We have also considered a generalization of the survival probability in which the “return position” is shifted from the average step position \bar{h} to an arbitrary reference

position R . The generalized (temporal) survival probability $S(t, R)$ is defined as the probability that the step position h is initially beyond the pre-assigned reference position, $h > R$ (or $h < -R$, for fluctuations that are symmetric about the average value, $\bar{h} = 0$), and remains there over a given time interval t . Clearly, $S(t, R = \bar{h}) = S(t)$, but the time-dependence of $S(t, R)$ for other values of R depends on the choice of R . Another generalization, the generalized inside survival probability $S_{in}(t, R)$, is defined as the probability of the step position remaining between the pre-assigned reference positions R and $-R$ (assuming the fluctuations to be symmetric about the average value, $\bar{h} = 0$) over time t .

Spatial persistence and survival probabilities are defined in the same way as the temporal quantities mentioned above, but considering the step position $h(x, t)$ to be a function of the coordinate x for fixed t . For example, the spatial persistence probability $P(x)$ is defined as the probability that the step position at a fixed time t does not return to its “initial” value $h(x_0, t)$ as one moves from the point x_0 to the point $x_0 + x$ along the average step direction (averages over x_0 and t are implied).

3. Models and numerical methods

If the separation between adjacent steps is sufficiently large, the entropic and elastic interactions [18, 19] between different steps may be neglected. We consider here this simple situation where the dynamics of a step is not affected by other steps on the surface. The energy of an isolated step is then simply proportional to the total length measured along its fluctuating edge. In a continuum description where the step-edge position is denoted by the function $h(x, t)$, the Hamiltonian of an isolated step is then given by

$$\begin{aligned} \mathcal{H}[h(x)] &= \tilde{\beta} \int_0^L [1 + |\partial h / \partial x|^2]^{1/2} dx \\ &\simeq \frac{\tilde{\beta}}{2} \int_0^L |\partial h / \partial x|^2 dx + \text{constant}, \end{aligned} \quad (1)$$

where $\tilde{\beta}$ is the “step-edge stiffness” (energy per unit length), L is the step size, and we have used a small-gradient expansion. At relatively high temperatures, fluctuations in the step position are known [14, 16, 41] to be dominated by random attachment and detachment (AD) of atoms at the step edge. The “noise” arising from these microscopic processes is clearly non-conserving: the total number of atoms in the crystal layer that terminates at the step edge does not remain constant when the AD mechanism is present. Under these conditions, the dynamics of step fluctuations is described by the second-order non-conserved linear Langevin equation

$$\frac{\partial h(x, t)}{\partial t} = \frac{\Gamma_a \tilde{\beta}}{k_B T} \frac{\partial^2 h(x, t)}{\partial x^2} + \eta(x, t). \quad (2)$$

Here, Γ_a is the “step mobility” and $\eta(x, t)$ is a non-conserved Gaussian noise satisfying $\langle \eta(x, t) \eta(x', t') \rangle = 2\Gamma_a \delta(x - x') \delta(t - t')$. This equation is known in the literature as the Edwards-Wilkinson (EW) equation [42]. In the dynamics governed

by this equation, the spatial average of the step position exhibits a random walk in time. In order to eliminate spurious effects of this random-walk behavior, we adopt the convention of measuring the step position from its instantaneous spatial average. Thus, from now on, the variable $h(x, t)$ will be used to denote the deviation of the step position at point x and time t from its spatial average at that time.

The AD mechanism freezes out at low temperatures and the primary mechanism of fluctuations in this regime is the step-edge diffusion (SED) of atoms [14, 16, 41]. The noise is clearly conserving in this case: the integral of $h(x, t)$ over the length of the step does not change as atoms diffuse along the step edge. Step edge fluctuations under these conditions are described by the fourth-order conserved Langevin equation

$$\frac{\partial h(x, t)}{\partial t} = -\frac{\Gamma_h \tilde{\beta}}{k_B T} \frac{\partial^4 h(x, t)}{\partial x^4} + \eta_c(x, t), \quad (3)$$

with $\langle \eta_c(x, t) \eta_c(x', t') \rangle = -2\Gamma_h \nabla_x^2 \delta(x - x') \delta(t - t')$. It is easy to check that Eqs.(2) and (3) lead to the same equilibrium behavior at long times, but due to the conserved nature of the noise, the dynamics governed by Eq.(3) strictly conserves the integral of $h(x, t)$ over x . The deterministic part of the Langevin equation (3) is the same as that in the so-called Mullins-Herring equation for surface growth [43], but the noise in the Mullins-Herring equation is non-conserving. In a general situation, both AD and SED may be present. However, theoretical studies [44, 45] suggest that a single mass transport mechanism will be dominant for most physical systems. Therefore, we can make the simplifying assumption of considering each mechanism separately, and study the dynamics governed by one of the two Langevin equations, (2) and (3).

All space and time-dependent correlation functions for these two linear Langevin equations can be calculated analytically. The equilibrium distribution of $h(x, t)$ is Gaussian with zero mean and width equal to the root-mean-square width of the step, $W(L) \propto L^\alpha$, with $\alpha = 1/2$. The mean-square difference in the step positions at two different points along the step at the same time is given by

$$G(x) \equiv \langle [h(x + x_0, t) - h(x_0, t)]^2 \rangle \propto x^{2\alpha}, \quad (4)$$

at equilibrium for $x \ll L$. Note that this dependence on x is the same as the dependence of the mean-square displacement on time in a 1d random walk. In fact, the spatial statistics of h in the equilibrium state is identical to the temporal statistics of the displacement in Brownian motion in one dimension.

Although the two Langevin equations considered here lead to the same equilibrium behavior, time-dependent correlations are different in the two cases. The equilibrium temporal correlation function of height fluctuations at the same point decays exponentially at long times,

$$C(t) \equiv \langle h(x, t_0 + t) h(x, t_0) \rangle \propto \exp[-t/\tau_c(L)], \quad (5)$$

where the correlation time $\tau_c(L)$ is proportional to L^z , with $z = 2$ for the EW equation and $z = 4$ for the conserved fourth-order equation. Also, the mean-square difference in the step positions at the same point at two different times is given by

$$G(t) \equiv \langle [h(x, t_0 + t) - h(x, t_0)]^2 \rangle \propto t^{2\beta}, \quad (6)$$

for $t \ll \tau_c$, with $\beta = \alpha/z$, so that $\beta = 1/4$ for the EW equation and $\beta = 1/8$ for the conserved fourth-order equation.

Although the step fluctuation $h(x, t)$ is a Gaussian stochastic variable, its non-Markovian nature makes analytic calculations of some of its first-passage properties difficult. In our studies, we used numerical integrations of the Langevin equations (2) and (3) to evaluate some of their temporal and spatial first-passage properties. In these numerical calculations, we used spatially discretized, dimensionless forms of the Langevin equations which were integrated forward in time using a simple Euler scheme. The dynamical equations considered in the numerical work are

$$\frac{dh_i}{dt} = (h_{i-1} + h_{i+1} - 2h_i) + \eta_i(t), \quad (7)$$

for the EW equation and

$$\frac{dh_i}{dt} = -(h_{i-2} - 4h_{i-1} + 6h_i - 4h_{i+1} + h_{i+2}) + \eta'_i(t), \quad (8)$$

for the conserved fourth-order equation. Here, $h_i(t)$ represents the step position at lattice site i at time t , $\eta_i(t)$ are uncorrelated random variables with zero mean and unit variance, and $\eta'_i(t)$ are the conserved version of such noise. Periodic boundary conditions were used in these calculations and results for different system sizes were obtained from averages over a large number of independent realizations of the stochastic time evolution.

In some of our numerical studies, we also used Monte Carlo simulations of the dynamics of 1d atomistic solid-on-solid models that are known to belong in the same dynamical “universality class” as the two Langevin equations mentioned above. For EW dynamics, we simulated the well-known Family model [46] in which atoms deposited randomly, one at a time, at the lattice sites are allowed to explore within a fixed diffusion length to find the lattice site with the smallest “height” h_j where it gets incorporated. If the diffusion length is one lattice constant (this is the value used in our simulations), the application of this deposition rule to a randomly selected site j involves finding the minimum value among the set h_{j-1}, h_j and h_{j+1} . The height of the site with the minimum height is then increased by one. Since the average height continues to grow in time in this model, the fluctuations of interest in the present context are obtained by subtracting the instantaneous spatial average from the variables $\{h_j\}$. An atomistic model proposed by Racz *et al.* [47] provides a discrete realization of the conserved dynamics of Eq.(3). In this model, the nearest-neighbor height differences are restricted to $|h_{j+1} - h_j| \leq 2$. In one simulation step, a site j is randomly chosen. A diffusion move to a randomly chosen neighbor takes place if the above restrictive condition is satisfied after the move; otherwise a new random site is selected and the procedure follows in the same way. In these atomistic simulations, “time” is measured in units of attempted depositions or moves per lattice site.

4. Experimental methods

The experimental results reviewed here were all extracted from variable-temperature scanning tunneling microscope (VT-STM) measurements of monatomic steps on solid surfaces. In this section, experimental concerns generic to all STM-based measurements of first-passage statistics are addressed. More specific details such as surface preparation and characterization can be found in Refs. [20, 21, 22, 28].

First passage measurements for surface steps have been performed under ultra-high vacuum conditions to allow for the preparation of surfaces with well-defined and reproducible structure and chemical composition. This level of control is crucial to the interpretation of experimental results in terms of theoretical models of interface fluctuations and also allows the use of repeated measurements on identically-prepared samples to reduce fluctuations in first-passage statistics. An important experimental demonstration that the surfaces are well-enough controlled is the measurement of the distribution (either temporal or spatial) of displacements of the step-edge. For an equilibrium system, the distribution must be Gaussian.

While STM is an obvious choice for real-space imaging experiments due to its remarkable spatial resolution, it is limited as a probe of dynamics by a relatively low data acquisition rate. For most surfaces with step edges that fluctuate rapidly enough to generate useful temporal statistics, it is not possible to obtain an STM image that corresponds to a snapshot of step configurations at a single instant of time. Therefore, the study of temporal step edge fluctuations often involves the use of so-called “line-scan” STM imaging. In this measurement, the STM tip is fixed at a point x_0 and scanned in one direction perpendicular to a step edge repeatedly for a fixed measurement time. An example of a resulting line-scan pseudo-image is shown in Fig. 1 and represents a time series of the evolution of the step position at x_0 . From this time series, $h(x_0, t)$, temporal first passage statistics can be extracted as described below.

The low speed of the STM creates different difficulties for the measurement of spatial first-passage statistics where snapshots corresponding to a given instant of time are required. To obtain these snapshots it is necessary to measure STM images at relatively low temperatures, where step fluctuations are slower than the rate of image acquisition, or to rapidly quench a surface from high temperature so that its step configuration is kinetically frozen [28, 48]. Once obtained, spatial STM images provide the step configuration at fixed time, $h(x, t_0)$, from which first-passage statistics may be extracted as a function of x . Experimentally determined spatial first-passage statistics have been found [31] to be noisier than the analogous temporal quantities. This arises partially due to the fact that, at large enough length scales along a step edge, there usually exist nonequilibrium features such as forced kinks due to small azimuthal crystal miscut or pinning sites due to trace contamination. Therefore, the fraction of a spatial image that can be considered for quantitative analysis is usually smaller than the fraction of a temporal pseudo-image.

The calculation of temporal persistence and survival from line-scan STM images

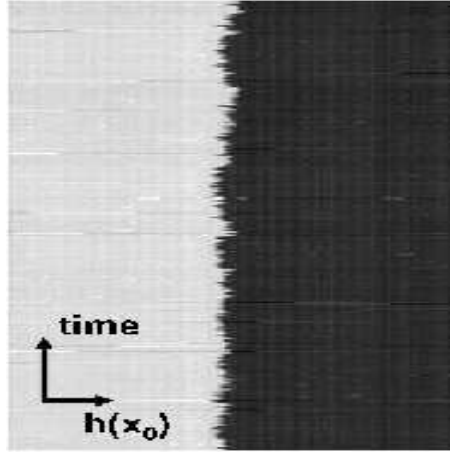


Figure 1. Example of line-scan pseudo-image of step fluctuations. In this figure, the step-edge position is denoted by h and x_0 denotes the coordinate in the average step direction.

proceeds differently than the calculation of these quantities from spatial images or from numerical simulations. In the latter two cases, probabilities are computed by calculating the fraction of all step sites that have not returned to the specified configuration (either as a function of time or of distance along the step). For line-scan STM data that is obtained at a single point on the step edge, however, probabilities must be computed by calculating the fraction of all time intervals for which the given step position has not returned to the specified configuration. For the measurements presented in the following sections, persistence and survival probabilities (as well as their generalizations) are computed from different STM images and averaged to obtain smooth curves that can be fit to theoretical predictions. Parameters from these fits, such as persistence exponents and survival decay constants, are quoted as the average obtained from the different measurements and the experimental error in the parameter is taken as the standard deviation (one σ) of the different measurements.

5. Analytic, numerical and experimental results

In this section, we present our results for various temporal and spatial first-passage properties of equilibrium step fluctuations quantified in terms of the persistence and survival probabilities defined in section 2. In each case, theoretical predictions (analytic when available and numerical) are compared with the results obtained from STM-based experiments for systems with different microscopic mechanisms of mass transport along the step edge.

5.1. Temporal persistence probabilities

For dynamics described by the linear Langevin equations (2) and (3), the step-edge fluctuation $h(x, t)$ at a fixed position x as a function of time t is a Gaussian stochastic

process, but it is not Markovian. The non-Markovian property arises from the presence of the spatial derivatives that generate “interactions” between height fluctuations at different space points. An exact analytic calculation of the persistence probability for a Gaussian but non-Markovian stochastic process is known [49] to be very difficult. In fact, the persistence probability $P(t)$ can not be meaningfully defined for the Langevin equations considered here if the time t is considered to be a truly continuous variable with no short-time cutoff. As discussed in section 2, $P(t)$ is defined in terms of the distribution of the time intervals between successive zero-crossings of the stochastic variable $Y(x, t) \equiv h(x, t_0 + t) - h(x, t_0)$, with $t_0 \gg \tau_c \propto L^z$. Time-displaced correlation functions of this quantity, which may be obtained from Eq.(6), involve the exponent β . It can be shown [33] that for $\beta < 1$, which is the case for the Langevin equations considered here, the density of zero crossings is infinite – once the process crosses zero, it immediately crosses zero again many times before making a long excursion to the next zero crossing. In this case, the persistence probability can be meaningfully defined only if a short-time cutoff is imposed. This, however, is not a serious problem because Langevin equations such as the ones considered here are to be understood as coarse-grained descriptions with naturally occurring short-time and short-distance cutoffs. Also, in experiments and simulations, the step position is measured at discrete time intervals, so that the smallest value of t for which $P(t)$ needs to be defined is the sampling interval δt . For this reason, there is no practical difficulty in measuring $P(t)$ in experiments and simulations, although the mathematical problem mentioned above implies that an exact analytic calculation of $P(t)$ for the models considered here is not possible.

It was shown in Ref. [33] that for linear Langevin equation of the type being considered here, the persistence probability $P(t)$ decreases in time as a power law, $P(t) \propto t^{-\theta}$, for $\tau_0 \ll t \ll \tau_c$ where τ_0 is short-time cutoff. It was also shown that the *persistence exponent* $\theta = 1 - \beta$, where β is the exponent defined in Eq.(6). This result was obtained from a scaling argument and confirmed by simulations. The scaling argument is based on the observation that the incremental autocorrelation function of the variable $Y(x, t)$ defined above has a power-law form with exponent β ,

$$\langle [Y(x, t_1) - Y(x, t_2)]^2 \rangle \propto |t_1 - t_2|^{2\beta}, \quad (9)$$

in the equilibrium state. This implies that the stochastic process $Y(x, t)$ is a *fractional Brownian motion* [50] with Hurst exponent β . For such a process, it is known that the probability that, given it has crossed zero at time $t = 0$, it returns to zero after time τ is proportional to $\tau^{-\beta}$, and $N(T)$, the total number of zero-crossings up to time T is proportional to $T^{1-\beta}$. Also, from the definition of the persistence exponent θ , it is clear that the number of zero-crossing intervals of length between τ and $\tau + d\tau$ in the total interval T is given by

$$n(\tau, T) \propto N(T) \tau^{-1-\theta} \propto T^{1-\beta} \tau^{-1-\theta}. \quad (10)$$

Using the relation,

$$\int_0^T d\tau \tau n(\tau, T) = T, \quad (11)$$

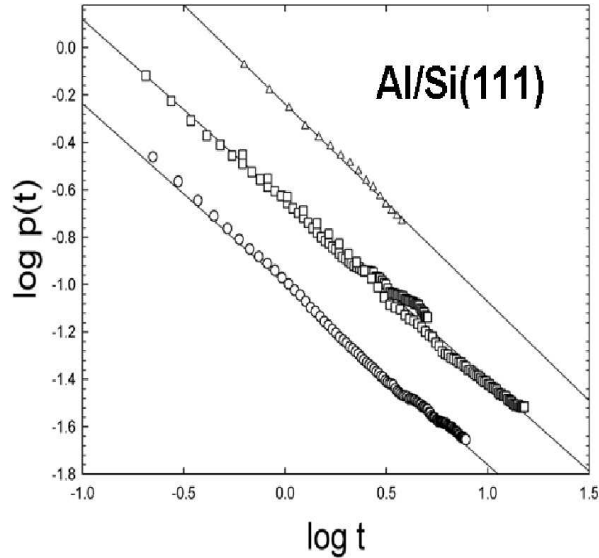


Figure 2. Double-logarithmic plots of the experimentally obtained persistence probability $p(t)$ for Al/Si(111) surface steps, as a function of time t , for three different temperatures (770K, 970K and 870K, from top to bottom). The plots have been offset vertically from one another for clarity of display (from Ref.[20]).

and equating powers of T on both sides of this equation, one then obtains the result, $\theta = 1 - \beta$. Simulations carried out in Ref. [33] and also by us have established the validity of this relation for the Langevin equations for step fluctuation. Therefore, the persistence exponent should be $\theta = 3/4$ for Eq.(2) and $\theta = 7/8$ for Eq.(3).

The first experimental study of temporal persistence probability for surface steps was carried out using measurements of step fluctuations on a vicinal surface of Si(111) modified by the adsorption of Al [20]. Previous experiments [48, 51] lead to the conclusion that the fluctuations in this system arise from the random exchange of mass between the step and the terrace and that the interface should therefore be modeled using the EW equation. Experimental persistence probabilities measured at three different temperatures for the Al/Si(111) surface steps are shown in Fig. 2. It is apparent from the linear behavior of the double-logarithmic plots that the persistence probability scales with time as a power law. The average persistence exponent for the Al/Si(111) surface is 0.77 ± 0.03 , in good agreement with the prediction of $\theta = 3/4$ for the EW equation.

Temporal persistence probabilities have also been extracted for metal surfaces of Pb(111) and Ag(111) where steps are known to fluctuate due to the SED mechanism [19, 52, 53]. The persistence probability has been found [21] to decay in time as a power law in these cases too. For steps on Pb(111), the persistence exponent is $\theta = 0.88 \pm 0.04$ and for steps on Ag(111), the persistence exponent is $\theta = 0.87 \pm 0.02$. These exponents are in agreement with the value of $7/8$ predicted for the conserved fourth-order Langevin

equation (3).

The most important role of these experimental results is to confirm the theoretical prediction of power law scaling of temporal persistence with an exponent that depends on the mass transport mechanism governing the relaxation of fluctuations. Furthermore, the experimental results quantitatively support the theoretically obtained relationship, $\theta = 1 - \beta$, between the persistence exponent θ and the more commonly measured growth exponent β . The persistence probability can therefore be used as an independent means of establishing the most appropriate model to describe a fluctuating interface.

We have also investigated the behavior of the probability of persistent large deviations $P(t, s)$, discussed in section 2, for step fluctuations. It was found in Ref. [39] that for a number of stochastic systems, the probability $P(t, s)$ decays in time as a power law, $P(t, s) \propto t^{-\theta_l(s)}$, with the exponent $\theta_l(s)$ varying continuously with s from $\theta_l(s) = \theta$, the usual temporal persistence exponent, for $s = 1$ to $\theta_l(s) = 0$ for $s = -1$. The function $\theta_l(s)$, $-1 \leq s \leq 1$, therefore, defines an infinite family of continuously varying exponents that characterizes the probability of persistent large deviations for the stochastic dynamical system under study. Analytic results for this function are available only for a class of simple spin models [54] in which the intervals between successive spin-flips are assumed to be uncorrelated. This assumption is not valid in the models of step fluctuation considered here. We have investigated [22] the behavior of $P(t, s)$ numerically and experimentally for step fluctuations with different mechanisms of microscopic mass transport.

For step fluctuations in a regime dominated by the AD mechanism, we have performed [22] numerical studies of the EW equation, Eq.(2), and the 1d Family model, and experiments on Al/Si(111) steps. In Fig. 3 we have shown three sets of results for $P(t, s)$, obtained from numerical integration of the EW equation, discrete stochastic simulation of the Family model, and analysis of the experimental data, respectively. It is clear that the decay of $P(t, s)$ at equilibrium follows a power law, $P(t, s) \propto t^{-\theta_l(s)}$, characterized by a persistent large deviation exponent $\theta_l(s)$ that varies continuously between 0 (for the limiting case $s = -1$) and the steady-state persistence exponent $\theta = 3/4$ (for the $s = 1$ case) discussed in the first part of this section. All three sets of results for the persistent large deviations exponents agree very well, establishing the infinite family of persistence exponents as a potentially powerful tool in studying dynamical interface fluctuation processes.

A similar set of exponents for persistent large deviations was also determined [22] from numerical studies of Eq.(3) and the atomistic model of Racz *et al.* described in section 3, and from Ag(111) step fluctuation measurements. The qualitative shape of the dependence of the experimentally obtained persistent large deviations exponent on the reference level s agrees well with the numerical results, but the quantitative agreement between numerical and experimental results in this case is not as good as it is for Al/Si(111). The reason for this discrepancy is not fully understood at present. There are some indications that the limited time range of experimental data or incomplete equilibration of numerical models might play a detrimental role to the correspondence

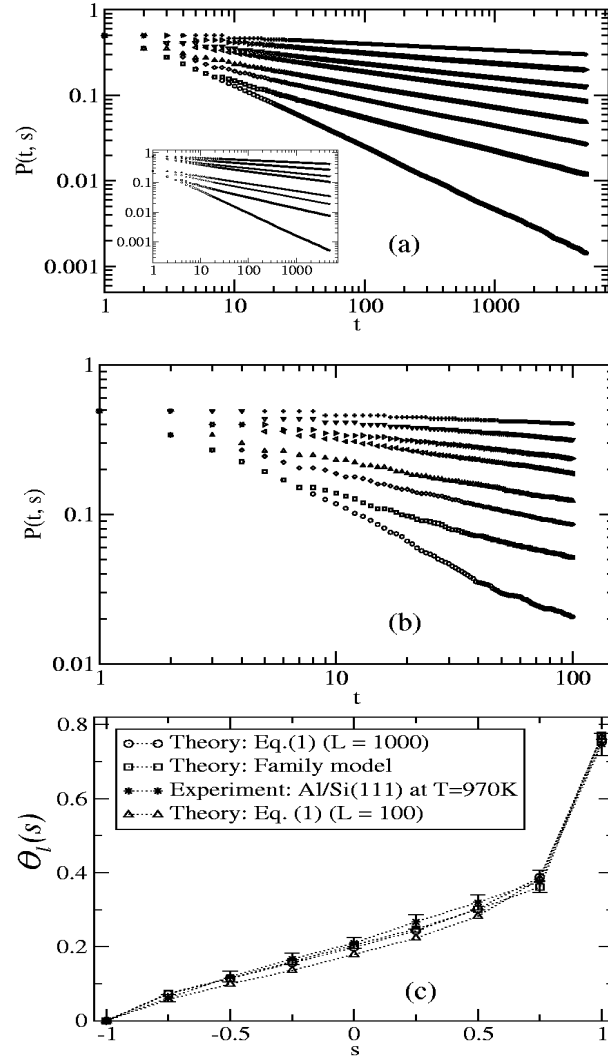


Figure 3. Log-log plots of $P(t, s)$ vs. t for high-temperature surface step fluctuations via the AD mechanism, shown for different values of s : $s = 1.0, 0.75, 0.5, 0.25, 0, -0.25, -0.5, -0.75$ (from the bottom to the top). (a) Eq.(2) (main figure) and the Family model (inset); (b) experimental data from STM step images of Al/Si(111) surface at 970K; and (c) comparison of the various sets of results for θ_l as a function of s . The error bars shown for the experimental data are obtained from variations of the local slope of the $\log P(t, s)$ vs. $\log t$ plots. Simulation results for two sample sizes are shown to illustrate that the use of small samples leads to an underestimation of $\theta_l(s)$ (from Ref. [22]).

between theory and experiment. A more intriguing possibility is that some aspects of mass transport on Ag(111) are not captured by the simplest form of the SED mechanism. This situation illustrates the potential value of investigating a broad range of statistical quantities, since all possible subtleties in fluctuation mechanisms may not be apparent from equilibrium correlation functions or even standard persistence probabilities.

5.2. Temporal survival probabilities

For step dynamics described by the linear Langevin equations (2) and (3), the equilibrium time-autocorrelation function of the fluctuations of the step position decays exponentially at long times (see Eq.(5)). This implies that $h(x, t)$ is a stationary Gaussian Process with exponentially decaying autocorrelation function. A well-known result [55] in the theory of stochastic processes then implies that the temporal survival probability $S(t)$ that measures the probability of $h(x, t)$ not crossing its average value $\bar{h} = 0$ over time t should also decay exponentially in time with a time constant τ_s that is proportional to the correlation time τ_c . The constant of proportionality $c = \tau_s/\tau_c$ is known to be less than unity and independent of the system size L , but its value is non-universal, being determined by the full functional form of the autocorrelation function $C(t)$. Thus, we arrive at the interesting result that although the definitions of the persistence probability $P(t)$ and the survival probability $S(t)$ appear to be quite similar, the fact that the reference levels used in their definitions are different (the initial step position for $P(t)$ and the average step position for $S(t)$) results in a qualitative difference in the long-time behaviors of these two quantities. Persistence probabilities convey, through the values of the persistence exponent θ and the infinite family of exponents $\theta_l(s)$ for persistent large deviations, information about the dynamical universality class of step fluctuations, whereas the survival probability conveys information about the long-time relaxation of step fluctuations. It should be noted that this difference arises from the continuous nature of the variable $h(x, t)$. Persistence and survival probabilities would be identical in problems involving discrete variables such as Ising spins for which a flip of the sign of a spin ensures a change of sign with respect to both initial and average values of the stochastic variable.

The exponential decay of $S(t)$ has been confirmed from simulations [23] and experiments [20, 28, 29] for both AD and SED dominated kinetics. Typical simulations results for $C(t)$ and $S(t)$ are shown in Fig. 4 (a-c) for dynamics governed by the EW equation. While the L -dependence of τ_c is known exactly, our results for $S(t)$ reveal the fact that although τ_s increases rapidly with L , as expected, there are clear deviations from the expected proportionality to L^z if the *sampling time* δt (i.e., the time between consecutive measurements of the step-edge position) is kept unchanged and only L is varied. Moreover, the scaling behavior of $S(t)$ can be revealed only if δt is carefully incorporated into the analysis. We explain in detail the important role played by the sampling time on the persistence and survival probabilities in the next subsection. Similar results were also obtained [23] for the fourth-order conserved Langevin equation, Eq.(3).

In Fig.5, the experimental survival probabilities and autocorrelation functions [20, 23] are shown for Al/Si(111) and Ag(111) on a semi-logarithmic plot. For both material systems, exponential decay is observed for temporal survival and autocorrelation even though the fluctuations on Al/Si(111) belong to a different model universality class than those on Ag(111). The detailed quantitative analysis of the survival probability depends

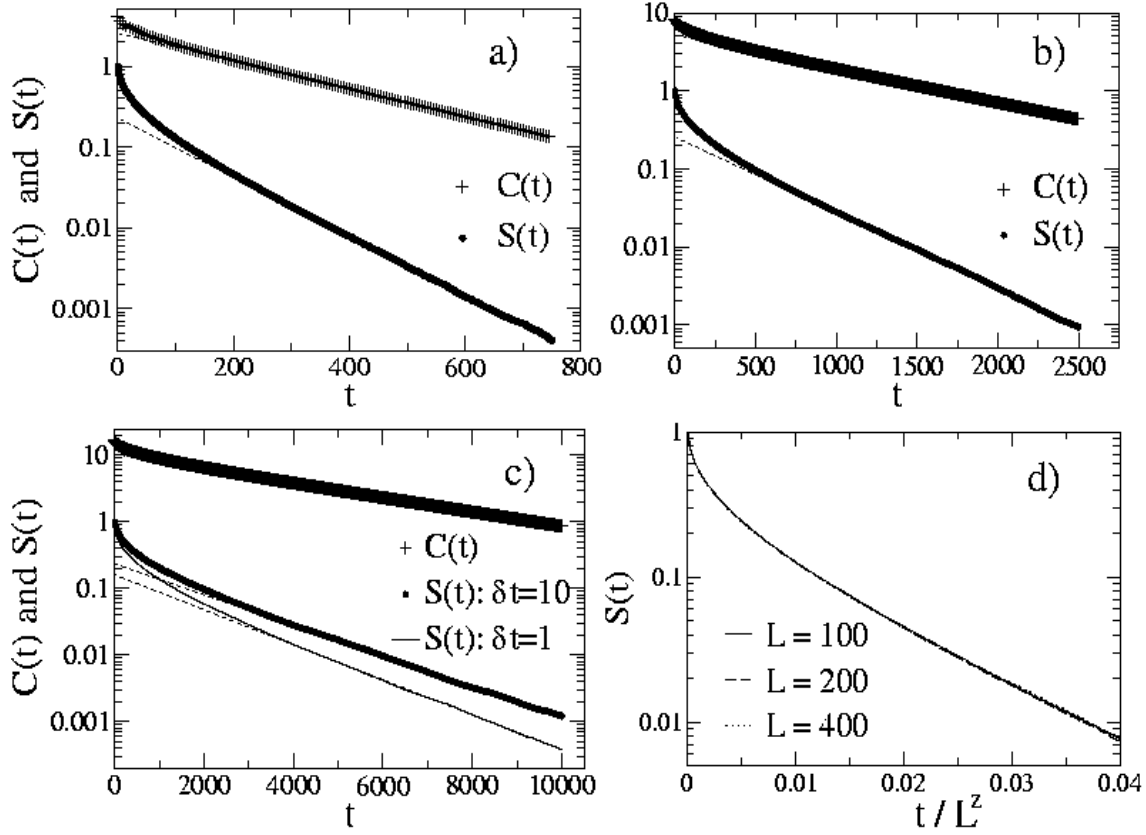


Figure 4. The survival probability $S(t)$ and the autocorrelation function $C(t)$ for the Langevin equation of Eq.(2). The dashed lines are fits of the long-time data to an exponential form. In panels (a-c), the uppermost plots show the data for $C(t)$. Panel (a): $L = 100$, $\delta t = 0.625$. Panel (b): $L = 200$, $\delta t = 2.5$. Panel (c): $L = 400$, $\delta t = 10.0$ (upper plot) and $\delta t = 1.0$ (lower plot). Panel (d): Finite-size scaling of $S(t, L, \delta t)$. Results for S for 3 different sample sizes with the same value of $\delta t/L^z$ ($z = 2$) are plotted versus t/L^z (from Ref. [23]).

on experimental subtleties arising from discrete sampling and finite measurement time. These issues will be discussed in the next subsection.

As noted in section 2, the temporal survival probability can be generalized [24] by considering probabilities associated with the interface position not crossing an arbitrarily chosen reference level R , as opposed to the equilibrium average position used in the definition of $S(t)$. This so-called generalized survival probability $S(t, R)$ is a natural means of addressing stability issues in nanostructured environments where the significant reference level is unlikely to be the precise equilibrium average interface position. For equilibrium step fluctuations, the generalized survival probability $S(t, R)$ is defined as the probability for the step position to remain consistently *above* a certain pre-assigned value R (or, equivalently, *below* $-R$, since the step fluctuations are symmetric about zero) over time t .

Numerical results [24] for the generalized survival probability and the associated time scale, obtained from simulations of the 1d Family model, are presented in Fig. 6.

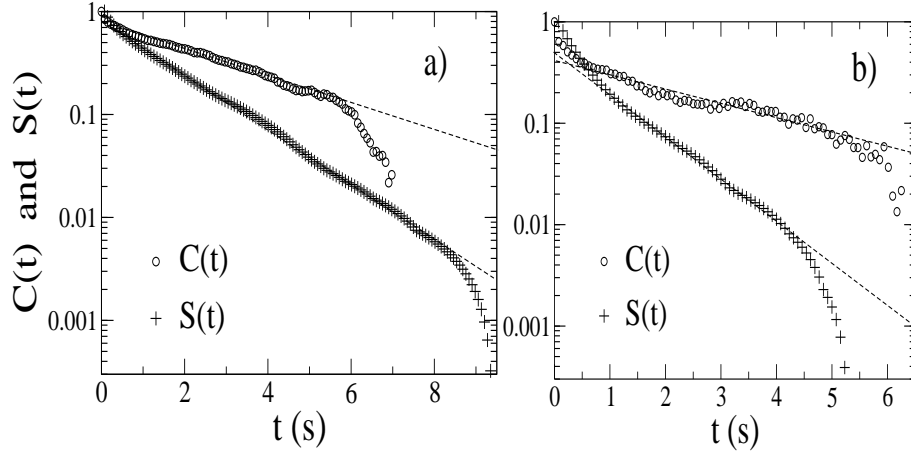


Figure 5. $S(t)$ and $C(t)$ for two experimental systems. The dashed lines are fits of the long-time data to an exponential form. Panel (a): Al/Si(111) at $T = 970\text{K}$. Panel (b): Ag(111) at $T = 450\text{K}$ (from Ref. [23]).

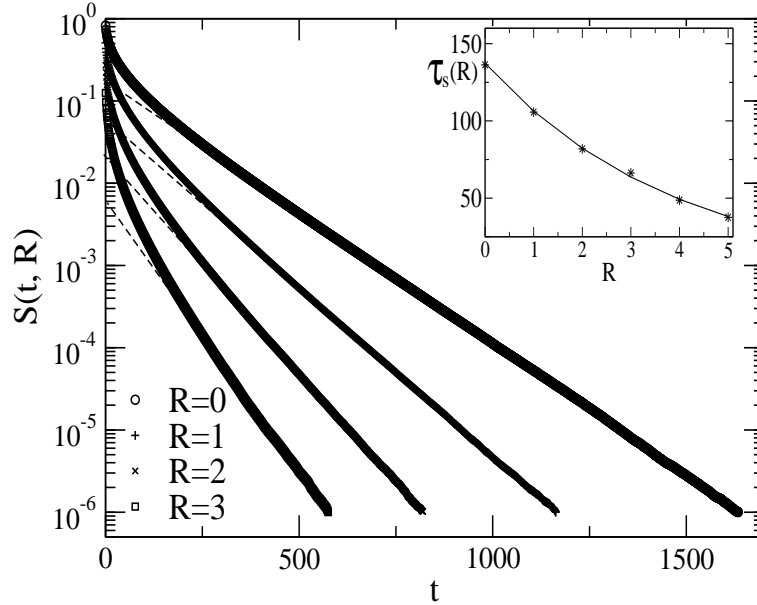


Figure 6. $S(t, R)$ for the discrete Family model. The dashed lines are fits of the long-time data to an exponential form. The system size is $L = 100$, the sampling time is $\delta t = 1.0$ and the reference level R takes four different values: 0, 1, 2 and 3 (from top to bottom). The inset shows the dependence of the generalized survival time scale $\tau_s(R)$ on the reference level value (up to $R = 5$). The continuous curve represents a fit to an exponential decay of $\tau_s(R)$ with R (from Ref. [24]).

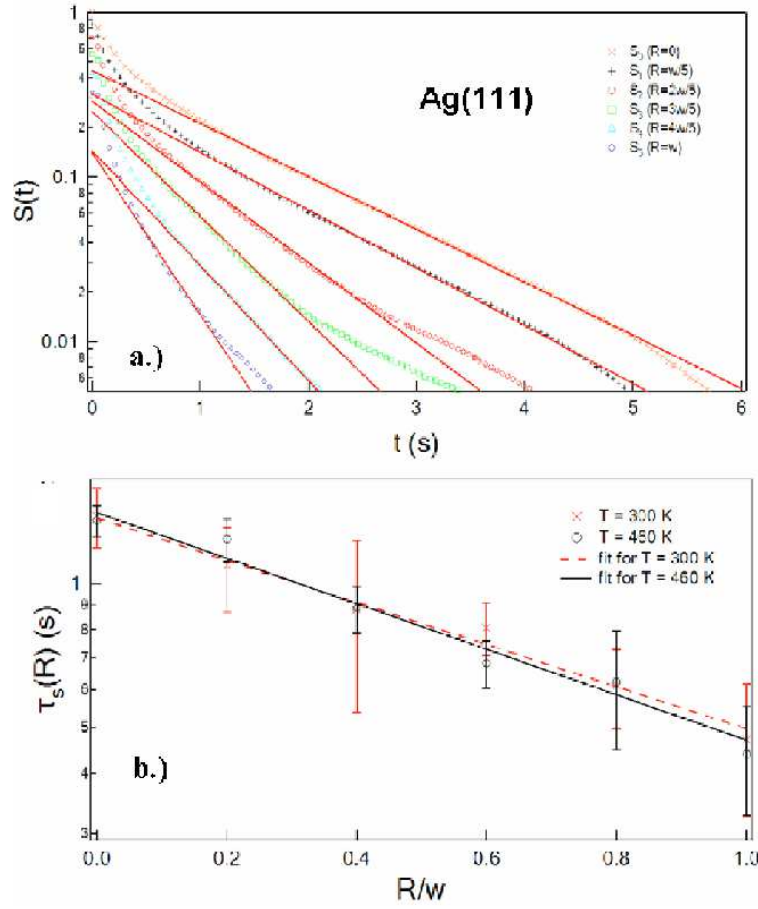


Figure 7. Experimental data (top panel) for the generalized survival probability $S(t, R)$ for Ag(111) steps. The bottom panel shows the variation of the time constant $\tau_s(R)$ with the scaling variable R/W where W is the measured root-mean-square fluctuation of the step position (from Ref. [32]).

For all R , $S(t, R)$ decays exponentially in the long-time limit, with an associated time scale, $\tau_s(R)$, which decreases with the reference level value. As shown in the inset of Fig. 6, the dependence of $\tau_s(R)$ on R appears to be exponential. At present, no analytic results are available for the time-dependence of $S(t, R)$ in the models being considered here.

Recently, the behavior of the generalized survival probability has been addressed [32] experimentally for the case of fluctuating steps on Ag(111) (kinetics governed by SED). The exponential decay of $S(t, R)$ in time for all values of R has been confirmed for this system, both through STM measurements and through numerical integration of the corresponding fourth-order conserved Langevin equation. The experimental data shown in the top panel of Fig. 7 suggest a scaling variable for the decay constant $\tau_s(R)$ in the form of the ratio of the chosen reference level R to the measured root-mean-square fluctuation W of the step position. Empirical fits to the dependence of $\tau_s(R)$ on R/W , shown in the bottom panel of Fig. 7 by the dashed lines,

suggest that the scaling function has a simple exponential form, in agreement with the simulation results for EW dynamics shown in Fig.6.

Finally, the generalized inside survival probability $S_{in}(t, R)$ defined in section 2 has also been studied numerically and experimentally [32] for step fluctuations governed by SED. Like the generalized survival probability, this quantity is expected to be a valuable characterization of stability and reliability in environments consisting of closely-spaced thermally fluctuating nanostructures. In both experiments and simulations, $S_{in}(t, R)$ is found to decay exponentially in time for all R . The time constant $\tau_{in}(R)$ of this decay scales with R/W , but the scaling function is different from that found for the generalized survival probability. In particular, it is found that $\tau_{in}(R)$ increases with R/W , and the dependence is not well-described by an exponential function. The experimental results for the time constant are found [32] to be in good agreement with numerical predictions when the effects of discrete sampling and finite observation time, discussed in detail in the next subsection, are taken into account.

5.3. Effects of discrete sampling, finite system size and finite observation time

As noted above, the step position $h(x, t)$ is measured in experiments and simulations at discrete intervals of a sampling time δt . It has been pointed out in Ref. [56, 57] that discrete-time sampling of a continuous-time stochastic process does affect the measured persistence and survival probabilities. Increasing the sampling interval increases the persistence and survival probabilities because some of the crossing events detected in sampling with a small δt are missed if the step position is sampled with a larger δt . The results shown in Fig. 4, panel (c) illustrate this important fact – the measured survival probability exhibits appreciable dependence on the value of δt . Also, simulations are always carried out for finite systems, and as explained below, the finiteness of the time over which measurements are carried out translates into a finite effective system size. Therefore, an understanding of the effects of the finiteness of the sample size L and the sampling time δt on the measured persistence and survival probabilities and their generalizations is crucial for extracting reliable values of parameters such as the persistence exponents and survival time scales from experiments and simulations.

We have used numerical simulations to examine in detail the effects of discrete sampling and finite system size on the measured first-passage probabilities. We have found [23, 24, 25] that the dependence of the measured persistence and survival probabilities on the sampling time δt and the system size L exhibits simple scaling behavior in terms of the dimensionless scaling variables $t/\tau_c(L)$ and $\delta t/\tau_c(L)$. This is reasonable, since the correlation time $\tau_c(L)$ is the only relevant time scale in these systems. The scaling behavior of the temporal survival probability is illustrated in Fig. 4, panel (d) where it is shown that plots of $S(t)$ versus the scaling variable $t/\tau_c(L)$ (recall that $\tau_c(L) \propto L^z$) for different L and δt all collapse to the same scaling curve if $\delta t/L^z$ is held fixed. These results are for the 1d EW equation for which $z = 2$. A similar scaling behavior was also found [23] for the survival probability for the fourth-order conserved

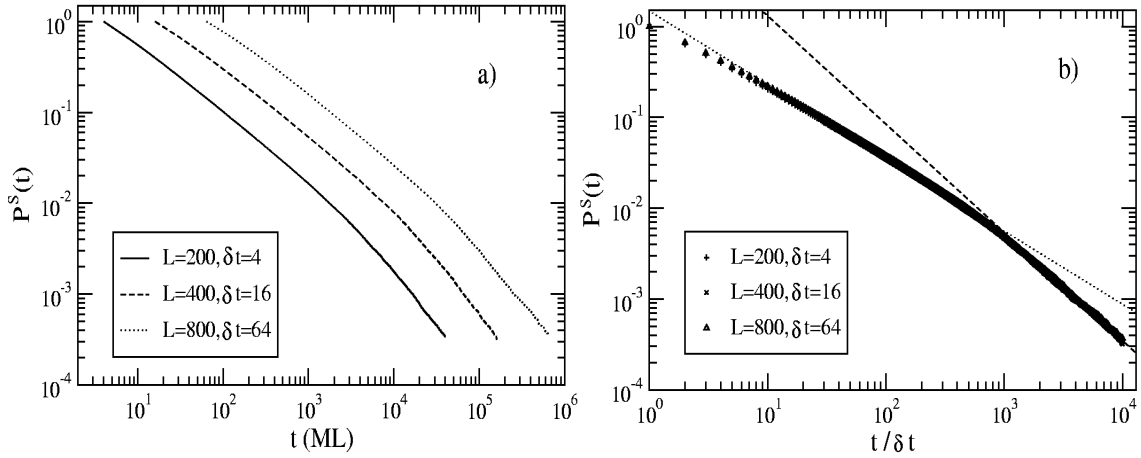


Figure 8. Persistence probability, $P(t)$, for the Family model shown for different system sizes with different sampling times. Panel a): Double-log plot showing three different $P(t)$ vs. time t curves corresponding to: $L = 200$ and $\delta t = 4$, $L = 400$ and $\delta t = 16$, $L = 800$ and $\delta t = 64$, from top to bottom, respectively. Panel b): Finite size scaling of $P(t, L, \delta t)$. Results for the persistence probabilities for three different sizes (as in panel a) with the same value of $\delta t/L^z$ (i.e. $1/10^4$) are plotted versus $t/\delta t$ ($z = 2$). The dotted (dashed) line is a fit of the data to a power law with an exponent $\simeq 0.75$ ($\simeq 1.0$) (from Ref. [25]).

Langevin equation of Eq.(3). From these results, we conclude that the dependence of the survival probability on the sampling interval and the sample size is described by the following scaling form:

$$S(t, L, \delta t) = f_S(t/L^z, \delta t/L^z), \quad (12)$$

where the function $f_S(x, y)$ decays exponentially for large values of x and the rate of this decay increases slowly as y is decreased.

We have found a similar scaling behavior for the steady-state persistence probabilities measured in our simulations:

$$P(t, L, \delta t) = f_P(t/L^z, \delta t/L^z), \quad (13)$$

where the scaling function $f_P(x, y)$ should decay as $x^{-\theta}$ for small x and $y \ll 1$. In Fig. 8, we show that the dependence of the steady-state persistence probability in the Family model ($z = 2$) on L and δt is described by this scaling form. Note that the scaling function f_P exhibits the expected power-law behavior for relatively small values of $t/\delta t$. However, we see signatures of a crossover to a power-law decay with exponent 1 as t approaches and exceeds the characteristic time scale $\tau_c(L) \propto L^z$. This behavior may be understood [25] from the fact that height fluctuations at two times separated by an interval that is much larger than τ_c are essentially uncorrelated. We have also shown [24] that the generalized survival probability $S(t, R)$ exhibits a similar scaling behavior. A non-zero value of the reference level R introduces a new length scale that is set by the equilibrium value of the interface width $W \propto L^\alpha$. Therefore, the scaling form of the

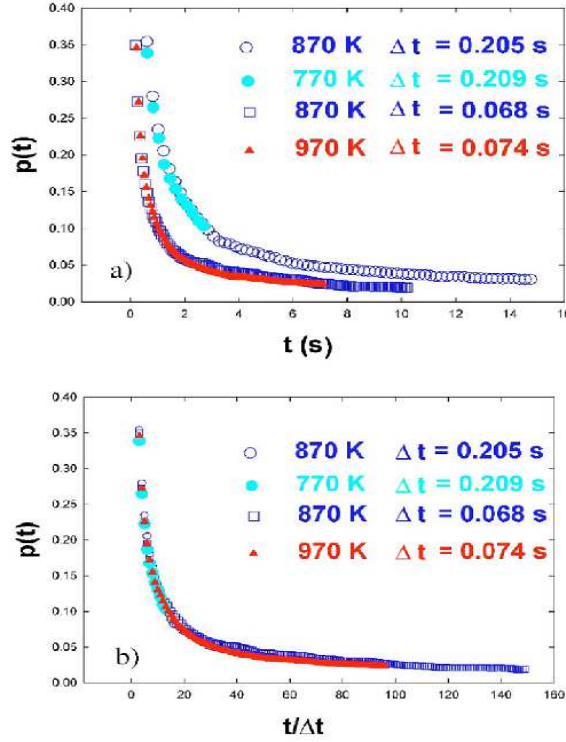


Figure 9. Experimentally determined persistence probabilities $P(t)$ for steps on Al/Si(111) are shown in panel (a) as a function of time t for different values of the temperature T and the sampling interval δt . The different curves collapse to the same one (panel (b)) when the persistence probabilities are plotted versus $t/\delta t$ (from Ref. [28]).

generalized survival probability is expected to be

$$S(t, L, R, \delta t) = g(t/L^z, R/L^\alpha, \delta t/L^z), \quad (14)$$

where the function $g(x, y, z)$ decays exponentially for large values of x . The validity of this scaling form for the generalized survival probability for the 1d Family model has been established in Ref.[24]. The use of the scaling variable R/W in the analysis of experimental data for generalized survival probabilities (see Fig. 7) is motivated by this scaling relation. The observed collapse of the data for $\tau_s(R)$ at two different temperatures to the same curve when plotted as a function of R/W (the values of W at the two temperatures are quite different) confirms the validity of the theoretically predicted scaling behavior.

Several other experimental observations [28, 29, 32] can be understood in terms of the effects of finite sampling interval and system size discussed above. Thermally-activated surface mass transport leads to strongly temperature-dependent linear kinetic parameters that enter as coefficients in the Langevin equations describing step motion [18, 19, 48]. This temperature dependence is readily apparent in experimentally-determined correlation functions. Remarkably however, experimental persistence and survival probabilities have not been observed to depend systematically on temperature.

This is due to the dependence of these quantities on the sampling interval and the (effective) sample size. The experimental situation for the persistence probability is illustrated in Fig.9 for Al/Si(111) step fluctuations [28]. It is seen from the data in panel (a) that when step positions are sampled with the same value of δt , persistence probabilities are indistinguishable even at very different temperatures. In panel (b), it is shown that the persistence probabilities from 770 K to 970 K collapse to the same curve when plotted versus time scaled by the sampling interval δt even though the underlying linear kinetic parameters vary by about two orders of magnitude [19]. This can be understood from the scaling relation of Eq.(13). Since the correlation time of the experimentally studied surface steps is much larger than the observation time, Eq.(13) implies that the measured persistence probability should depend only on the scaled time $t/\delta t$: in this regime, the sampling interval sets the overall normalization of the persistence probability. It is important to point out that this discrete sampling “artifact” does not affect the shape of the persistence probability (i.e the value of the persistence exponent) but only its absolute magnitude. This behavior is likely to be found in the measurement of any first-passage probability using a sampling rate slower than the underlying physical processes and must be considered carefully in analyzing experimental data.

In experimental studies of temporal survival probabilities, another “artifact” arises from the finiteness of the total measurement time t_m . This is because definitions of survival probabilities require the value of the average step position \bar{h} : the temporal survival probability measures the probability of the step position not returning to \bar{h} , and the reference level R in measurements of the generalized survival probability is defined relative to \bar{h} . In analytic and numerical studies, \bar{h} is known to be equal to zero. In experiments, however, \bar{h} is set to be equal to the average of the step position measured over the time interval t_m . This average is generally not the “true” average step position because fluctuation modes with relaxation times much larger than t_m do not equilibrate during the observation time which is limited by the lateral stability of the microscope. Analytic and numerical calculations described in Ref. [29] show that the main effect of the finiteness of t_m is very much similar to that of having a finite effective system size $L_{eff} \propto t_m^{1/z}$, with $z = 2$ for AD dominated kinetics and $z = 4$ for SED limited kinetics. Using this result (i.e. setting $L = L_{eff}(t_m)$) in the scaling relations (12) and (14) that describe the dependence of survival probabilities on the system size, one obtains new scaling relations that describe the expected dependence of the experimentally measured survival probabilities on the sampling interval δt and the measurement time t_m . These scaling relations involve the scaling variables t/t_m and $\delta t/t_m$. The validity of these scaling relations has been established [29, 32] from experimental measurements of the temporal survival probability and the generalized survival probability for different values of sampling time and observation time. For example, it has been shown in Ref. [29] that for steps on Ag(111), plots of the survival probability versus $t/\delta t$ for different values of t_m and δt collapse to the same scaling curve only when the ratio $\delta t/t_m$ is held fixed. Since the effective system size is limited by the observation time t_m , the time scales

for the decay of the measured autocorrelation function of step-edge fluctuations and the related survival probabilities are all expected to be of order t_m . This explains why the measured first-passage properties do not show any systematic dependence on the temperature.

5.4. Spatial persistence and survival probabilities

Spatial counterparts of the temporal persistence and survival probabilities may be defined by considering the equilibrium profile $h(x, t)$ of a step at a fixed time t as a function of x . The spatial persistence probability $P(x_0, x_0 + x)$ is simply the probability that $h(x, t)$ *does not* return to its “original” value $h(x_0, t)$ at the initial point x_0 within a distance x measured from x_0 along the average step direction. In the statistically time-independent equilibrium state, this probability does not depend on t . A theoretical study [58] of this probability for Gaussian interfaces with dynamics described by linear Langevin equations shows that its dependence on x has a power-law form with an exponent that depends on how the initial point x_0 is selected. If x_0 is sampled uniformly from *all* the points of a steady-state interface configuration, then the average of $P(x_0, x_0 + x)$ over x_0 yields the *steady-state* spatial persistence probability $P_{SS}(x)$ that decays with x as a power law with an exponent θ_{SS} ($P_{SS}(x) \propto x^{-\theta_{SS}}$) known as the steady-state spatial persistence exponent. If, on the other hand, the initial point x_0 is sampled from a subset of points of a steady-state configuration for which the values of $h(x, t)$ and its spatial derivative are finite, then the so-called *finite-initial-conditions* spatial persistence probability is obtained, which decays with x as a power law with an exponent that may be different from θ_{SS} . The values of these exponents for interfaces with dynamics described by a class of linear Langevin equations have been determined in Ref. [58] using a mapping of the spatial statistical properties of the interface to the temporal properties of stochastic processes described by a generalized random-walk equation. Steady-state and finite-initial-conditions spatial survival probabilities are defined in a similar way in terms of the probability of the interface not crossing its average value over distance x .

We have carried out numerical studies [26] of these spatial first-passage probabilities for the models of equilibrium step fluctuation described in section 3. Both steady-state and finite-initial-conditions probabilities defined above were considered in these studies. For brevity, we describe below the results obtained for the steady-state spatial persistence and survival probabilities. Since the equilibrium spatial properties are the same for the two Langevin equations (2) and (3), we consider only the EW equation and the Family model that belongs in the same universality class.

As discussed in section 3, the incremental spatial autocorrelation function of the variable $h(x, t)$ in the equilibrium state exhibits a power-law behavior with exponent $\alpha = 1/2$ (see Eq.(4)). It is, therefore, clear that the incremental spatial autocorrelation function of the variable $Z(x, t) \equiv h(x_0 + x, t) - h(x_0, t)$, whose zero-crossing statistics determines the spatial persistence probability $P_{SS}(x)$, also exhibits a power-law behavior

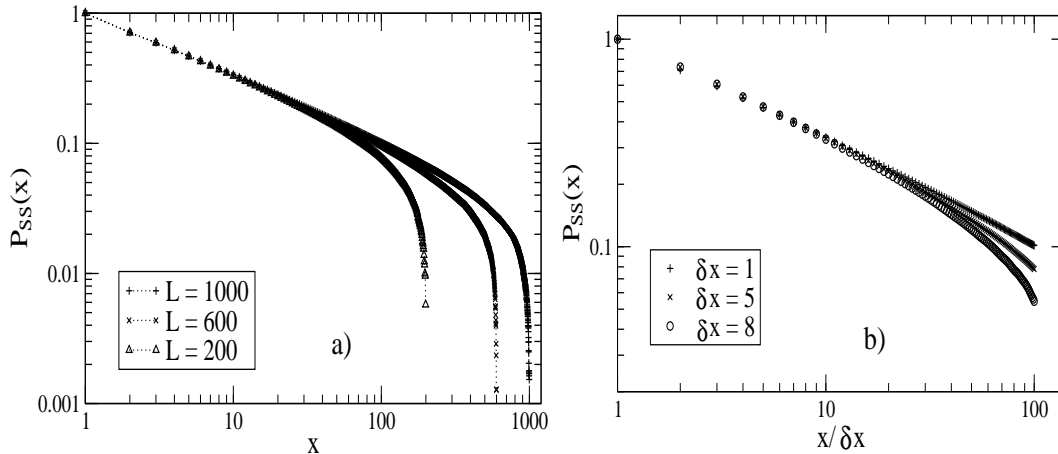


Figure 10. The steady state spatial persistence probability, $P_{SS}(x)$, for EW interfaces, obtained using the discrete Family model. Panel (a): Double-log plots of $P_{SS}(x)$ vs x for a fixed sampling distance $\delta x = 1$, using three different values of L , as indicated in the legend. Panel (b): Double-log plots of $P_{SS}(x)$ vs $x/\delta x$ for a fixed system size, $L = 1000$, and three different values of δx , as indicated in the legend (from Ref. [26]).

with the same exponent:

$$\langle [Z(x_1, t) - Z(x_2, t)]^2 \rangle \propto |x_1 - x_2|^{2\alpha}. \quad (15)$$

Comparing this with Eq.(9) and using arguments identical to those used for obtaining the relation between the temporal persistence exponent θ and the dynamical exponent β , one readily obtains the result that the steady-state spatial persistence exponent for EW interfaces is given by $\theta_{SS} = 1 - \alpha = 1/2$. This result also follows from the exact mapping [58] between the spatial statistics of a steady-state EW interface and the temporal statistics of Brownian motion. This mapping implies that the spatial persistence exponent θ_{SS} for a steady-state EW interface is equal to the temporal persistence exponent, $\theta = 1/2$, for Brownian motion.

This behavior of the steady-state spatial persistence probability has been confirmed [26] from simulations of the Family model. Two length scales have to be taken into consideration in the interpretation of the numerical results: the size L of the sample used in the simulation, and the sampling distance δx which denotes the spacing between two successive points where the height variables are measured in the calculation of the persistence probability. The minimum value of δx is obviously one lattice spacing, but one can use a larger integral value of δx in the calculation of persistence and survival probabilities. Examples of the effects of finite L and δx in simulation results for the Family model are shown in Fig. 10. The plots in panel (a) show that for $P_{SS}(x)$ measured in systems with different sizes, using the smallest possible value for δx (i.e. $\delta x = 1$), the exponent associated with the power-law decay of the persistence probability does not change, but there is an abrupt downward departure from power-law behavior near $x = L/2$. In panel (b), we have shown the results for $P_{SS}(x)$ when L remains fixed and δx is varied. Since the persistence probability is, by definition, equal to unity for

$x = \delta x$, we have plotted P_{SS} as a function of $x/\delta x$ in this figure to ensure that the plots for different values of δx coincide for small values of the x -coordinate. The plots for different δx are found to splay away from each other at large values of $x/\delta x$, with the plots for larger δx exhibiting more pronounced downward bending. The numerical results [26] indicate that the dependence of $P_{SS}(x)$ on L and δx exhibits a scaling behavior similar to that found for the temporal persistence and survival probabilities:

$$P_{SS}(x, L, \delta x) = f_{SS}(x/L, \delta x/L), \quad (16)$$

where the function $f_{SS}(x_1, x_2)$ shows power-law decay with exponent θ_{SS} as a function of x_1 for small values of x_1 and $x_2 \ll 1$. Fits of the numerical data to a power-law yields $\theta_{SS} \simeq 0.51$, in good agreement with the expected value of $1/2$. The probability of persistent large deviations of spatial fluctuations and the associated family of exponents can be defined in analogy with their temporal counterparts. These exponents for 1d EW interfaces have been obtained in Ref.[27] using simulations of the Family model. As expected, the dependence of the spatial persistent large deviations exponent on the parameter s is found to be identical to that of the temporal persistent large deviations exponent for 1d Brownian motion.

Numerical results obtained in Ref.[26] indicate that for 1d EW interfaces at equilibrium, the dependence of the steady-state spatial survival probability $S_{SS}(x)$ on x is not described by exponential or power-law forms over a large range of x values. Simulations for different sample sizes and different values of the sampling interval δx reveal that the survival probability is a function of the scaling variable x/L , and that its dependence on δx is weak. These numerical results have been explained in a recent analytic study [30] in which one of the authors was involved. This study makes use of the exact mapping of the spatial statistics of 1d EW interfaces at equilibrium to the temporal statistics of 1d Brownian motion. The effects of periodic boundary conditions used in the simulations and the fact that $h(x, t)$ is measured relative to its instantaneous spatial average (so that the integral of $h(x, t)$ over x from $x = 0$ to $x = L$ is strictly equal to zero) are taken into account in this calculation. Using an exact path integral formulation, it has been shown that $S_{SS}(x, L)$ is a function of x/L , and an exact expression for this function in term of complicated integrals that can, in principle, be evaluated has been obtained. A simpler closed-form expression for this function was also obtained in Ref. [30] from a simple “deterministic” approximation and it was shown that the results obtained from this calculation agree very well with those of simulations.

Spatial first-passage properties of equilibrium step fluctuations governed by the AD mechanism have also been measured [31] for the Al/Si(111) system. As mentioned earlier, experimental systems display a dramatic temperature dependence due to thermally activated kinetics. As a result, it is possible to decrease the rate of step fluctuations to an immeasurably slow value, yielding a static spatial step structure that represents an equilibrium configuration frozen in time. For the Al/Si(111) system, fluctuations are essentially absent over time intervals of several minutes for temperatures below 770 K [59], while at 1020 K steps fluctuate with times scales of the order

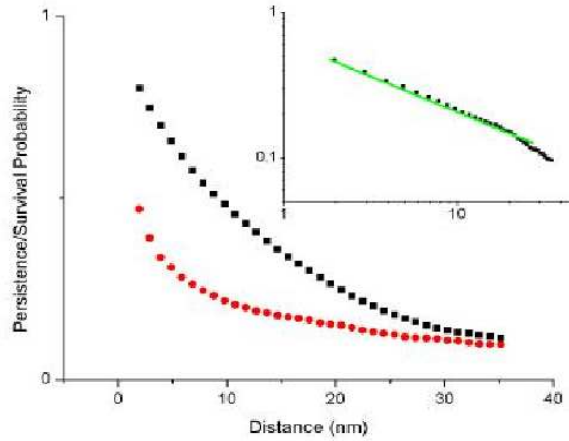


Figure 11. Representative spatial persistence and survival probability data. The data were taken at 970 K, from an STM image with pixel size of 0.977 nm. The persistence and survival probabilities are represented by squares and circles respectively. The inset is the same persistence curve using logarithmic scales. The solid green line is a power law fit to the data over the linear region with the steady-state spatial persistence exponent $\theta_{SS} = 0.59$ (from Ref. [31]).

of seconds [48]. Therefore, to obtain viable information above 870 K, samples were prepared at elevated temperatures and were then quenched at an initial cooling rate of over 200 K/s to room temperature in order to capture and preserve the step-edge displacements [59]. In measurements of spatial first-passage properties, the spatial separation between adjacent measured points (or pixel size) plays the role of the sampling distance δx mentioned above.

Spatial persistence and survival probabilities were measured for Al/Si(111) surfaces representing spatial equilibrium over temperatures of 720–1070 K. The images used in these measurements were of two sizes, $(300 \text{ nm})^2$ and $(500 \text{ nm})^2$, measured with pixel sizes 0.586 nm and 0.977 nm respectively. Each step image used for this analysis was cropped from a larger original STM image, yielding a distribution of effective system sizes L but the same value of the pixel size δx . Experimental data were analyzed to determine both the spatial persistence and survival probabilities versus distance x , as shown in Fig. 11. The same persistence curve is shown in the inset using logarithmic axes to illustrate more clearly the power-law behavior. Deviations from the power-law fit at large distances stem from limited statistics at large x , as well as possible effects of finite measurement size issues. The average of the persistence curves for all the steps in each image was fit to a power law to extract the persistence exponent θ_{SS} . No systematic dependence on temperature was observed, similar to the lack of temperature-dependence observed for the temporal persistence. An analysis of the averaged persistence probabilities over all the temperatures results in a persistence exponent of $\theta_{SS} = 0.498 \pm 0.062$, in excellent agreement with the theoretical value

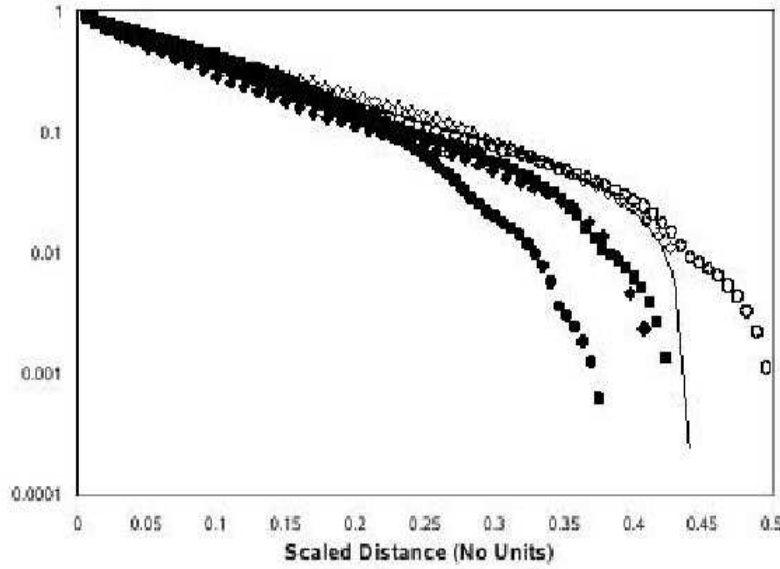


Figure 12. Survival probabilities determined from single steps chosen to display measurements at two different pixel sizes and a wide range of step lengths. Solid diamonds, squares, and circles are from $(500 \text{ nm})^2$ images and have system lengths of $L = 98.9 \text{ nm}$, 170 nm , and 162 nm respectively. Open diamonds, squares, and circles are from $(300 \text{ nm})^2$ images and have system lengths of $L = 65.8 \text{ nm}$, 154 nm , and 87 nm respectively. The survival probability is plotted as a function of the scaled distance x/L . The solid line represents the theoretical prediction of Ref.[30] (from Ref. [31]).

of $1/2$.

The measured survival curves $S_{SS}(x)$ showed a great deal of variability, but scaling the distance x by the length L of the step caused the curves to collapse onto one another, as illustrated in Fig. 12. No systematic effect of the ratio $\delta x/L$ on the linear region of the semi-logarithmic plots in Fig. 12 was observed. Fits of the scaled survival probabilities to an exponential form gave good results for short distances ($x/L < 0.2$), with an average value of the scaled decay length $x_s/L = 0.076 \pm 0.033$ with a temperature-dependence smaller in magnitude than the experimental uncertainty in the data. The fit of the short-distance survival data to an exponential form with a fixed decay length is, in fact, consistent with the short-distance form of the theoretical prediction [30] for the spatial survival probability of 1d EW interfaces. The theoretically predicted survival probability, shown as the solid line plotted in Fig. 12, reproduces the rapid fall-off of the survival probability at larger distances. Consistent with the experimental observation, the functional form is indistinguishable from an exponential for $x/L < 0.2$, except very close to $x = 0$ where the theoretical result predicts a cusp of the form $S_{SS}(u) \sim 1 - 4\sqrt{3u}/\pi$ with $u = x/L$. The empirical survival length constant x_s/L extracted from exponential fits is a useful experimental rule of thumb that provides a measure of the characteristic fluctuation length scales relative to the system size.

6. Summary and discussions

The theoretical and experimental results summarized above provide a fairly complete description of temporal and spatial first-passage properties of the equilibrium fluctuations of isolated steps on a surface. The close agreement between theoretical (analytic when available and numerical) and experimental results in nearly all the cases studied provides a confirmation of several theoretical ideas about first-passage properties of dynamical fluctuations of spatially extended objects, validates the simple theoretical models used to describe these fluctuations, and establishes the usefulness of first-passage statistics in characterizing the nature of these fluctuations. Due to the non-Markovian nature of these fluctuations, it is difficult to carry out analytic calculations of some of the first-passage probabilities considered here. In particular, no analytic theory is available at present for the family of persistent large deviations exponents $\theta_l(s)$ and the time scales for the decay of the generalized survival probability $S(t, R)$ and the generalized inside survival probability $S_{in}(t, R)$. The development of analytic theories for these quantities would be very interesting and useful.

The results reviewed above also indicate that in general, the issues of discrete sampling, finite measurement time, and finite effective step length make the interpretation of non-universal aspects of persistence and survival data for step fluctuations a difficult prospect. These difficulties do not detract from the remarkably successful interplay between experiment and theory that has enhanced fundamental understanding of the statistical physics of model 1d interfaces. Nevertheless, since first-passage statistics speaks to eminently practical concerns related to structural stability, the interpretation of measurements in a material and temperature dependent context is crucial. We have shown that the dependence of first-passage probabilities on sampling parameters and effective step length can be quantified in terms of phenomenological scaling relations obtained using plausible arguments and confirmed from numerical studies. The development of a deeper (analytic if possible) understanding of these scaling relations would be very useful in extracting quantitative information from experimental studies of first-passage properties.

The studies described here may be extended in several directions. Most nonlinear models [60, 61, 62, 63] used to describe the nonequilibrium kinetics of surface growth do not have the $h \rightarrow -h$ symmetry of the linear models considered here. This lack of symmetry translates into a difference between the exponents [25, 34] that describe the decay of steady-state temporal persistence probabilities for positive and negative displacements of the interface from its initial position. The smaller of these two persistence exponents is known [25] to be equal to $(1 - \beta)$ where β is the dynamical growth exponent of the nonlinear model, but no analytic result is available for the other exponent. Also, it has been found in simulations [25, 33, 34] that “transient” persistence exponents that describe the temporal first-passage statistics in the initial regime of interface growth from a flat initial state are different from the steady-state persistence exponents. Studies of some of the other first-passage properties considered in our

work for these situations would be interesting. Other interesting questions that deserve attention include the effects of step-step interactions on the first-passage properties of step fluctuations and persistence and survival properties of higher-dimensional interfaces such as fluctuating membranes and growing surfaces in two dimensions.

Acknowledgments

We would like to thank O. Bondarchuk, B. R. Conrad, W. G. Cullen, M. Degawa, I. L. Lyubinetsky, S. N. Majumdar, P. Punyindu Chatrathorn and C. G. Tao for their contributions in some of the studies described here. We would also like to thank S. N. Majumdar and J. Krug for helpful discussions. CD would like to thank the Condensed Matter Theory Center, Laboratory for Physical Sciences of the University of Maryland for support and hospitality during a sabbatical visit. This work was supported by the Condensed Matter Theory Center of the University of Maryland and UMD NSF-MRSEC under Grant No. DMR 05-20471.

References

- [1] S. Redner, *A Guide to First-passage Processes* (Cambridge University Press, Cambridge, 2001).
- [2] S. N. Majumdar, *Curr. Sci.* **77**, 370 (1999).
- [3] S. N. Majumdar, C. Sire, A. J. Bray, and S. J. Cornell, *Phys. Rev. Lett.* **77**, 2867 (1996); B. Derrida, V. Hakim, and R. Zeitak, *Phys. Rev. Lett.* **77**, 2871 (1996).
- [4] B. Derrida, V. Hakim, and V. Pasquier, *Phys. Rev. Lett.* **75**, 751 (1995).
- [5] S. N. Majumdar and C. Sire, *Phys. Rev. Lett.* **77**, 1420 (1996).
- [6] S. N. Majumdar, A. J. Bray, S. J. Cornell and C. Sire, *Phys. Rev. Lett.* **77**, 3704 (1996).
- [7] D.S. Fisher, P Le Doussal and C. Monthus, *Phys. Rev. Lett.* **80**, 3539 (1998).
- [8] M. Constantin and S. Das Sarma, *Phys. Rev. E* **72**, 051106 (2005).
- [9] M. Marcos-Martin, D. Beysens, J. P. Bouchaud, C. Godreche, and I. Yekutieli, *Physica A* **214**, 396 (1995).
- [10] W. Y. Tam, R. Zeitak, K. Y. Szeto, and J. Stavans, *Phys. Rev. Lett.* **78**, 1588 (1997); W. Y. Tam and K. Y. Szeto, *Phys. Rev. E* **65**, 042601 (2002).
- [11] B. Yurke, A. N. Pargellis, S. N. Majumdar, and C. Sire, *Phys. Rev. E* **56**, R40 (1997).
- [12] G. P. Wong, R. W. Mair, and R. L. Walsworth, *Phys. Rev. Lett.* **86**, 4156 (2001).
- [13] J. Merikoski, J. Maunuksela, M. Myllys, J. Timonen, and M. J. Alava, *Phys. Rev. Lett.* **90**, 024501 (2003).
- [14] A. -L. Barabasi and H. E. Stanley, *Fractal Concepts in Surface Growth* (Cambridge University Press, Cambridge, 1995).
- [15] J. Krug, *Adv. Phys.* **46**, 139 (1997).
- [16] A. Pimpinelli and J. Villain, *Physics of Crystal Growth* (Cambridge University Press, Cambridge, 1998).
- [17] C. Misbah, O. Pierre-Louis, and Y. Saito, to be published (2007).
- [18] H.-C. Jeong and E. D. Williams, *Surf. Sci. Reports* **34**, 171 (1999).
- [19] M. Giesen, *Prog. Surf. Sci.* **68**, 1 (2001).
- [20] D. B. Dougherty, I. L. Lyubinetsky, E. D. Williams, M. Constantin, C. Dasgupta, and S. Das Sarma, *Phys. Rev. Lett.* **89**, 136102 (2002).
- [21] D. B. Dougherty, O. Bondarchuk, M. Degawa, and E. D. Williams, *Surf. Sci.* **527** L213 (2003).
- [22] M. Constantin, S. Das Sarma, C. Dasgupta, O. Bondarchuk, D. B. Dougherty, and E. D. Williams, *Phys. Rev. Lett.* **91**, 086103 (2003).

- [23] C. Dasgupta, M. Constantin, S. Das Sarma, and S. N. Majumdar, Phys. Rev. E **69**, 022101 (2004).
- [24] M. Constantin and S. Das Sarma, Phys. Rev. E **69**, 052601 (2004).
- [25] M. Constantin, C. Dasgupta, P. Punyindu Chatraphorn, S. N. Majumdar, and S. Das Sarma, Phys. Rev. E **69**, 061608 (2004).
- [26] M. Constantin, S. Das Sarma, and C. Dasgupta, Phys. Rev. E **69**, 051603 (2004).
- [27] M. Constantin and S. Das Sarma, Phys. Rev. E **70**, 041602 (2004).
- [28] D. B. Dougherty, C. Tao, O. Bondarchuk, W. G. Cullen, E. D. Williams, M. Constantin, C. Dasgupta, and S. Das Sarma, Phys. Rev. E **71**, 021602 (2005).
- [29] O. Bondarchuk, D. B. Dougherty, M. Degawa, E. D. Williams, M. Constantin, C. Dasgupta, and S. Das Sarma, Phys. Rev. B **71**, 045426 (2005).
- [30] S. N. Majumdar and C. Dasgupta, Phys. Rev. E **73**, 011602 (2006).
- [31] B. R. Conrad, W. G. Cullen, D. B. Dougherty, I. Lyubinetzky, E. D. Williams, Physical Rev. E, in press (2007).
- [32] C. G. Tao, W. G. Cullen, E. D. Williams and C. Dasgupta, submitted (2007).
- [33] J. Krug, S. N. Majumdar, S. J. Cornell, A. J. Bray, and C. Sire, Phys. Rev. E **56**, 2702 (1997).
- [34] H. Kallabis and J. Krug, Europhys. Lett **45**, 20 (1999).
- [35] J. Krug, Physica A **340**, 647 (2004).
- [36] V.V. Zhirnov and R.K. Cavin, Nature Materials **5**, 11 (2006).
- [37] G. K. Ramachandran, T. J. Hopson, A. M. Rawlett, L. A. Nagahara, A. Primak, and S. M. Lindsay, Science **300**, 1413 (2003).
- [38] B. Q. Xu and N. J. J. Tao, Science **301**, 1221 (2003).
- [39] I. Dornic and C. Godreche, J. Phys. A **31**, 5413 (1998).
- [40] T. J. Newman and Z. Toroczkai, Phys. Rev. E **58**, R2685 (1998); Z. Toroczkai, T. J. Newman, and S. Das Sarma, Phys. Rev. E **60**, R1115 (1998).
- [41] N. C. Bartelt, J. L. Goldberg, T. L. Einstein, and Ellen D. Williams, Surf. Sci. **273**, 252 (1992).
- [42] S. F. Edwards and D. R. Wilkinson, Proc. R. Socs. London, Ser.A **381**, 17 (1982).
- [43] W. W. Mullins, J. Appl. Phys. **28**, 333 (1957); C. Herring, J. Appl. Phys. **21**, 301 (1950).
- [44] S.V. Khare and T.L.Einstein, Phys. Rev. B **57**, 4782 (1998).
- [45] T. Ihle, C. Misbah, and O. Pierre-Louis, Phys. Rev. B **58**, 2289 (1998).
- [46] F. Family, J. Phys. A: Math. Gen. **19**, L441 (1986).
- [47] Z. Racz, M. Siegert, D. Liu, and M. Pliscke, Phys. Rev. A **43**, 5275 (1991).
- [48] I. L. Lyubinetzky, D. B. Dougherty, T. L. Einstein, and E. D. Williams Phys. Rev. B **66**, 085327 (2002).
- [49] D. Slepian, Bell Syst. Tech. J. **41**, 463 (1962).
- [50] B. B. Mandelbrot and J. W. van Ness, SIAM Rev. **10**, 422 (1968).
- [51] D.B. Dougherty, I. Lyubinetzky, T.L. Einstein, and E.D. Williams, Phys. Rev. B **70**, 235422 (2004).
- [52] L. Kuipers, M.S. Hoogeman, J.W.M. Frenken, and H. van Beijeren, Phys. Rev. B **52**, 11387 (1995).
- [53] S. Speller, W. Heiland, A. Biederman, E. Platzgummer, C. Nagl, M. Schmid, and P. Varga, Surf. Sci. **331**, 1056 (1995).
- [54] A. Baldassarri, J. P. Bouchaud, I. Dornic, and C. Godreche, Phys. Rev. E **59**, R20 (1999).
- [55] G. F. Newell and M. Roseblatt, Ann. Math. Stat. **33**, 1306 (1962).
- [56] S. N. Majumdar, A. J. Bray and G. C. M. A. Ehrhardt, Phys. Rev. E **64**, 015101 (2001).
- [57] G. C. M. A. Ehrhardt, A. J. Bray, and S. N. Majumdar, Phys. Rev. E **65**, 041102 (2002).
- [58] S. N. Majumdar and A. J. Bray, Phys. Rev. Lett. **86**, 3700 (2001).
- [59] I. Lyubinetzky, D. B. Dougherty, H. L. Richards, T. L. Einstein, and E. D. Williams, Surf. Sci. **492**, L671 (2001).
- [60] M. Kardar, G. Parisi, and Y. -C. Zhang, Phys. Rev. Lett. **56**, 889 (1986).
- [61] S. Das Sarma and P. Tamborenea, Phys. Rev. Lett. **66**, 325 (1991); P. Tamborenea and S. Das

- Sarma, Phys. Rev. E **48**, 2575 (1993).
- [62] D. Wolf and J. Villain, Europhys. Lett. **13**, 389 (1990).
- [63] C. Dasgupta, S. Das Sarma, and J. M. Kim, Phys. Rev. E **54**, R4552 (1996); C. Dasgupta, J. M. Kim, M. Dutta, and S. Das Sarma, Phys. Rev. E **55**, 2235 (1997).